Long-lasting antinociceptive effects of green light in acute and chronic pain in rats

Mohab M. Ibrahim[a,b,1,*,+], **Amol Patwardhan**[a,b,1], **Kerry B. Gilbraith**[a], **Aubin Moutal**[b], **Xiaofang Yang**[b], **Lindsey A. Chew**[b], **Tally Largent-Milnes**[b], **T. Philip Malan**[a,b], **Todd W. Vanderah**[a,b], **Frank Porreca**[a,b,¶], and **Rajesh Khanna**[b,*,¶,+]

[a]Department of Anesthesiology, College of Medicine, University of Arizona, Tucson, AZ 85742, USA

[b]Department of Pharmacology, College of Medicine, University of Arizona, Tucson, AZ 85742, USA

Keywords

green-light phototherapy; constellation pharmacology; calcium imaging; proteomics; neuropathic pain; thermal antinociception; mechanical allodynia

1. Introduction

In the USA, over 100 million patients suffer from chronic pain [36]. On average, 261–300 billion dollars are spent annually to manage pain and 297–336 billion dollars are lost to work nonproductivity [36]. Additionally, the emotional tax from chronic pain has resulted in life altering events ranging from shattering family unity [72] to suicide attempts [26; 29; 32]. Options for treatment of acute, post-operative pain as well as for chronic pain are limited and many drugs are marginally effective [22] and often accompanied by severe side-effects [19]. Non-pharmacological options for the treatment of pain would be highly desirable and advantageous in terms of safety, including lack of tolerance, somnolence, addiction, gastrointestinal disturbances and perhaps other factors such as convenience and cost.

Light therapy has been reported to be useful for multiple medical conditions. For example, light therapy, has been used to control depression [20; 25], to increase daytime circadian stimulation, and to improve sleep quality and mitigate depression in Alzheimer's disease [21]. Additionally, bright light improved the mood of adolescents taking antidepressants compared to those without light therapy [61]. Exposing patients to bright light of more than

[*]To whom correspondence should be addressed: Mohab M. Ibrahim, M.D., Ph.D., Department of Anesthesiology, College of Medicine, University of Arizona, 1501 North Campbell Drive, P.O. Box 245050, Tucson, AZ 85724, USA Office phone: (520) 626-4281; Fax: (520) 626-2204; mibrahim@anesth.arizona.edu; Rajesh Khanna, Ph.D., Department of Pharmacology, College of Medicine, University of Arizona, 1501 North Campbell Drive, P.O. Box 245050, Tucson, AZ 85724, USA Office phone: (520) 626-4281; Fax: (520) 626-2204; rkhanna@email.arizona.edu.
[1]co-first authors
[+]These authors contributed equally.
[¶]Rajesh Khanna and Frank Porreca are co-senior authors.

6000 lux significantly improved seasonal affective disorder (SAD), a serious condition with increased risk of suicidality [20; 25]. Pain has sensory, cognitive and affective dimensions [9; 58]. The emotional state of patients significantly influences pain [24]. For example, chronic psychological stress and depression increased pain perception in humans when painful and non-painful heat stimulus were applied to their forearms [76]. A similar response is also reported in rodents. In a model of social defeat, rats demonstrated enhanced nociceptive response to subcutaneous formalin administration [2]. In contrast, elevated emotional status may decrease the perception of pain [46]; general happiness and laughter therapy significantly decreased chronic pain scores in elderly patients [79]. Similar findings were observed in primary care patients who were enrolled in positive psychological intervention programs, which decreased their depression and improved overall functionality, as well as decreased pain perception [42]. It is possible that light therapy may have psychological effects, possibly arising from physiological changes such as increased endogenous opioid release, as shown in this study, which affect pain response or its perception.

Few studies have investigated possible effects of light therapy on pain. A randomized clinical trial investigated the effect of bright light exposure in managing nonspecific back pain where patients received once a week light exposure for 3 weeks reduced pain as assed by the Brief Pain Inventory suggesting an active role for light in controlling pain [43]. Preclinical studies on the possible modulation of pain by light therapy have not been reported. Here, we investigated the effect of light in modulation of acute nociception as well as in a model of chronic neuropathic pain. We found that green light produced antinociceptive and antihyperalgesic effects that involved descending, opioid-sensitive inhibition.

2. Methods

2.1. Animals

Pathogen-free, adult male and female Sprague–Dawley as well as male Long Evans rats (weight at testing 250–350 g; Harlan–Sprague–Dawley, Indianapolis, IN) were housed in a climate-controlled room on a 12-h light/dark cycle and were allowed to have food and water ad libitum. All procedures were approved by the University of Arizona Animal Care and Use Committee and conform to the guidelines for the use of laboratory animals of the National Institutes of Health (publication no. 80–23, 1966). All behavioral experiments were conducted by experimenters blinded to the treatment conditions. The experiments were replicated a minimum of two times with independent cohorts of animals.

2.2. Chemicals

All experimental compounds, doses, sources, and catalog numbers are described in Table 1.

2.3. Light Emitting Diodes (LED)

All visible spectrum LED flex strips were purchased from ledsupply.com (VT, USA). The specification of the LED were: (*i*) #LS-AC60-6-BL, 472 nanometer wavelength (i.e., blue), 8 watts, 120 Volts, 120 degree beam angle; (*ii*) #LS-AC60-6-GR, 525 nanometer wavelength

(i.e., green), 8 watts, 120 Volts, 120 degree beam angle; and (*iii*) #LS-AC60-66-WH, white, 9.6 watts, 120 Volts, 120 degree beam angle. LED strips were affixed to the outside of clear plastic cages that housed the rats so as to avoid the strips from being chewed. Rats were exposed to the various LED in these cages with full access to food and water in a dark room devoid of any other source of light. Following behavioral assessment, the rats were returned to their cages for additional LED exposure. At the end of daily testing, the rats were returned to their regular animal room where they were exposed to room light (regular florescent bulbs). A lux meter (Tondaj LX1010B, Amazon.com) was used to determine the illuminance and luminous emittance of the LED strips.

Since there are no previously published data reporting the effects of green LED on antinociception in rats, as a first step, we performed 'pilot' experiments using a fixed amount (330 lux – which represents one full 'strip') of green LED over time noting that antinociception developed only after 3 to 5 hours of exposure for at least three days. This antinociception continued to gradually increase over the next two days of exposure, reaching its zenith between days 4 and 5 (data not shown). The bulk of the studies were thus performed with 8 hours daily exposure for 5 days. Next, we performed a light intensity versus antinociception analysis, which revealed that lower lux intensity was more effective than higher lux exposure for 8 hours daily for 5 days. These pilot experiments formed the basis of the exposure paradigm used in these studies – lux level, number of hours of exposure per day, and number of days of exposure.

2.4. Thermal sensory thresholds

Paw withdrawal latencies were determined as described by Hargreaves et al. [28] was used. Rats were acclimated within Plexiglas enclosures on a clear glass plate maintained at 30°C. A radiant heat source (high-intensity projector lamp) was focused onto the plantar surface of the hind paw. When the paw was withdrawn, a motion detector halted the stimulus and a timer. A maximal cutoff of 33.5 sec was used to prevent tissue damage.

2.5. Tactile thresholds

The assessment of tactile sensory thresholds was determined by measuring the withdrawal response to probing the hindpaw with a series of calibrated fine (von Frey) filaments. Each filament was applied perpendicularly to the plantar surface of the paw of rats held in suspended wire mesh cages. Withdrawal threshold was determined by sequentially increasing and decreasing the stimulus strength (the "up and down" method), and data were analyzed with the nonparametric method of Dixon, as described by Chaplan *et al.* [12] and expressed as the mean withdrawal threshold.

2.6. Elevated plus maze (EPM)

The EPM consists of four elevated (50cm) arms (50cm long and 10cm wide) with two opposing arms containing 30cm high opaque walls. EPM testing occurred in a quiet testing room with ambient lighting at ~500 lux. On day of testing, rats were allowed to acclimate to the testing room for 20 minutes. Each rat was placed in a closed arm, facing the enter platform and cage mates started in the same closed arm. Each rat was allowed 5 minute to explore the EPM and then returned to its home cage. Between animals the EPM was cleaned

thoroughly with Versa-Clean (Fisher Scientific). EPM performance was recorded using an overhead video camera (MHD Sport 2.0 WiFi Action Camera, Walmart.com) for later quantification. Open and closed arm entries were defined as the front two paws entering the arm, and open arm time began the moment the front paws entered the open arm and ended upon exit. An anxiety index was also calculated; the index combines EPM parameters into one unified ratio with values ranging from 0 to 1, with a higher value indicating increased anxiety [34]. The following equation was used for calculation of the anxiety index:

$$\text{Anxiety index} = 1 - (\text{open arm time}/5 \text{ min}) + (\text{open arm entry}/\text{total entry}).$$

2.7. Implantation of intrathecal catheters

For intrathecal drug administration, rats were implanted with catheters as described by Yaksh and Rudy [83]. Rats were anesthetized with isoflurane and placed in a stereotactic device. The occipital muscles were separated from their occipital insertion and retracted caudally to expose the cisternal membrane at the base of the skull. Polyethylene tubing was passed caudally from the cisterna magna to the level of the lumbar enlargement. Animals were allowed to recover and were examined for evidence of neurologic injury. Animals with evidence of neuromuscular deficits were excluded.

2.8. Fabricating rat contact lenses and imaging of eyes post-mortem

All plastic materials were purchased from Evergreen Scale Models (Des Plaines, Illinois). We used the method developed by Levinson et al [71], with the following modifications. In brief, 0.25mm sheets were cut into 2cm^2 pieces held by forceps over a 6mm ball bearing, shaped when malleable with a copper pipe of 9 mm internal diameter and then trimmed in to a truncated hemisphere with iris scissors and sanded with a fine grit and emery cloth to a depth of 3.5 ± 0.2mm and a base diameter of 7.0 ± 0.2mm. We used a Wellar 1095-1000watt dual temperature heat gun, instead of the Bunsen burner used by Levinson, as a heat source for the fabrication process. The rats where anesthetized using isoflurane just long enough to place the contact lens in their eyes and were allowed to recover from anesthesia. The rats were anesthetized again with isoflurane to remove the contact lens at the end of each 8 hour exposure.

To examine if the contact lens induced any pathological damage, at the end of the experiment, the corneas were excised with the small rim of the sclera and then fixed for 30 minutes with 4% paraformaldehyde in phosphate buffered saline as described previously [63]. Next, the corneas were transferred to 30% sucrose solution until staining with Evans blue solution for 1 min. The Evans blue dye solution was prepared by mixing 1 ml of a commercially prepared 0.5% Evans blue sterile aqueous solution with 9 ml of normal saline. This yielded a final solution of 0.05 % Evans blue, with a pH of 6.75. After staining, the excess dye was removed by gently passing the tissue through two baths of normal saline solution. Light microscope images were obtained of the stained corneas on an Olympus BX51 microscope with a Hamamatsu C8484 digital camera using a 4× UplanFL N, 0.13 numerical aperture or a 20× UplanSApo 0.75 numerical aperture objective. The freeware

image analysis program Image J (http://rsb.info.nih.gov/ij/) was used to generate merged images.

2.9.1 Spinal nerve ligation (SNL)—Nerve ligation injury produces tactile allodynia and thermal hypersensitivity [40]. All nerve operations occurred 5 days after intrathecal catheter implantation. Rats were anesthetized with 2% isoflurane in O_2 anesthesia delivered at 2 L/min (total time under anesthesia was < 60 minutes). The skin over the caudal lumbar region was incised and the muscles retracted. The L_5 and L_6 spinal nerves were exposed, carefully isolated, and tightly ligated with 4-0 silk distal to the dorsal root ganglion without limiting the use of the left hind paw of the animal. All animals were allowed 7 days to recover before any behavioral testing. Any animals exhibiting signs of motor deficiency were euthanized. Sham control rats underwent the same operation and handling as the SNL animals, but without the nerve ligation.

2.9.2. Rostral ventromedial medulla (RVM) cannulation—Rats received a bilateral guide cannula (26GA,#C235-1.2mm, Plastics One Inc.) directed to the RVM. The cannula was placed at: −11.0 from bregma, −7.5mm from the dura and 0.6mm on either side of the midline. Injections were made by expelling 0.5 μl through an injection cannula protruding 1 mm beyond the tip of the guide. Cannula placement was confirmed with 0.5μl Evans Blue injected into both sides of the cannula and microscopic examination of medullary sections and data from rats with misplaced cannula were eliminated from the experiment. Acute single injections into the RVM were performed by inserting an injector (Plastics One Inc #C235I-SPC) attached to a 2μl Hamilton syringe and expelling 0.5μl at the same coordinates.

2.10. Rotarod

Rats were trained to walk on a rotating rod (10 rev/min; Rotamex 4/8 device) with a maximal cutoff time of 180 seconds. Training was initiated by placing the rats on a rotating rod and allowing them to walk until they either fell off or 180 seconds was reached. This process was repeated 6 times and the rats were allowed to recover for 24 hours before beginning green LED exposure. Prior to treatment, the rats were run once on a moving rod in order to establish a baseline value. Assessment consisted of placing the rats on the moving rod and timing until either they fell off or reached a maximum of 180 seconds.

2.11.1. Samples preparation for proteomics—DRG and dorsal horn of the spinal cord from rats exposed to ambient light or GLED (4 lux, 5 days, 8 hours/day) were isolated and lysates were prepared as described above. Proteins were precipitated using 100% ice-cold acetone and centrifuged at 15000×g at 4°C for 10 min. The pellets, containing solubilized proteins, were re-suspended in 100mM Tris pH=7.4, 8M urea (to eliminate carrying forward any salt contamination) and their protein content analyzed by mass spectrometry at the Arizona Proteomics Consortium after trypsin digestion.

2.11.2. Database searching—Tandem mass spectra were extracted. Charge state deconvolution and deisotoping were not performed. All MS/MS samples were analyzed using Sequest (Thermo Fisher Scientific, San Jose, CA, version 1.3.0.339). Sequest was set

up to search RattusNorvegicus_UniprotKB_2016_0406_cont.fasta assuming the digestion enzyme trypsin. Sequest was searched with a fragment ion mass tolerance of 0.80 Da and a parent ion tolerance of 10.0 PPM. Oxidation of methionine and carbamidomethyl of cysteine were specified in Sequest as variable modifications.

2.11.3. Criteria for protein identification—Scaffold (version 4.5.1, Proteome Software Inc., Portland, OR) was used to validate MS/MS based peptide and protein identifications. Peptide identifications were accepted if they could be established at greater than 20.0% probability to achieve a false discovery rate (FDR) less than 0.1% by the Scaffold Local FDR algorithm. Protein identifications were accepted if they could be established at greater than 100.0% probability and contained at least 5 unique peptides. Protein probabilities were assigned by the Protein Prophet algorithm [59]. Proteins that contained similar peptides and could not be differentiated based on MS/MS analysis alone were grouped to satisfy the principles of parsimony. Proteins sharing significant peptide evidence were grouped into clusters. Proteins were annotated with gene ontology (GO) terms from gene_association.goa_uniprot [3].

2.12. Semi quantitative real time polymerase chain reaction

Semi quantitative real time polymerase chain reaction (qRT-PCR) was performed as described previously [8; 56]. After GLED treatment or control, rat spinal cords were dissected and the lumbar region isolated before flash freezing in liquid N_2. The cords were kept at −80°C until analysis. RNA was extracted from tissues using Tri reagent (Cat# TR118, MRC, Cincinnati, OH) according to the manufacturer's protocol. Briefly, Tri reagent was added to the cords before homogenization. The homogenates were centrifuged at 5000 × g for 5 min at 4°C to eliminate insoluble materials, then chloroform was added to the supernatants at 20 % (v/v). After centrifugation at 12000×g for 15 min at 4°C, the upper, RNA containing, aqueous fraction was harvested in a new tube and total RNA was subsequently precipitated by adding isopropanol (50 %, v/v). The precipitates were subjected to a final centrifugation at 20000×g for 10 min at 4°C and the RNA pellets were washed twice with 75% ethanol. Finally, purified RNA was resuspended in ultra-pure water and stored at −20°C until analysis. To generate cDNA, 2 μg of purified RNA were retrotranscribed using Maxima Reverse Transcriptase (Cat# EP0743, Thermo Fisher) according to the manufacturer's instructions. qRT-PCR analysis was performed using 5X HOT FIREPol Evagreen (Cat# 08-24-00020, Solis Biodyne, Estonia) on a CFX connect (Biorad, Hercules, CA) according to manufacturer's instructions. Specific primer sequences used are in Table 2. L27 expression was measured as a housekeeping gene to normalize target mRNA expression between samples. The relative mRNA level for each gene (x) relative to L27 mRNA (internal control) was calculated using the   Ct method [48].

2.13. Data analysis

The statistical significance of differences between means was determined by parametric analysis of variance (ANOVA) followed by post hoc comparisons (Student-Newman-Keuls test) using GraphPad Software. Animal numbers required to achieve statistical power for each *in vivo* experiment were determined by G.Power3.1, using post-hoc variance estimates from pilot experiments. Pharmacological profiling of sensory neurons data was analyzed

using Sigma Plot 12.5 and compared by z-test. Differences were considered to be significant if p ≤ 0.05. All data were plotted in GraphPad Prism 6.

3. Results

3.1. Antinociceptive effects of GLED

We first determined if various kinds of light conditions affected responses to a noxious thermal stimulus in naïve rats. Rats were exposed, for eight hours, to ambient room light that consisted of white fluorescent lights and ambient sunlight through glass windows (600 lux), white LED (575 lux), or darkness (0 lux) and paw withdrawal latency (PWL) was measured immediately after termination of illumination. As shown in Fig. 1, the PWLs were unchanged across all conditions. In contrast, naïve rats exposed to GLED (525 nm wavelength; 110 lux) for eight hours daily for five days demonstrated a time-dependent increase in PWL that was significantly higher than rats exposed to ambient room light. Testing was done immediately after termination of GLED (Fig. 1). PWLs were also higher in rats exposed to blue LED (472 nm wavelength; 110 lux) but less than in those rats exposed to GLED (Fig 1). The increase in PWLs, elicited by GLED exposure (Fig. 2A), plateaued by the second day and was unchanged thereafter until the fifth day (Fig. 2B). The GLED exposure was terminated on day 5 and the PWLs were measured on subsequent days to determine if the increase in PWLs was transient or long-lasting. The increase in PWLs induced by GLED exposure was maintained for 4 days before returning to baseline (Fig. 2B).

The preceding experiments were conducted with 110 lux GLED. However, whether this lux level was sufficient to elicit the antinociceptive behavior is not known. Consequently, we exposed the rats to GLED spanning several lux intensities. Exposing rats for eight hours to 4 lux GLED levels was sufficient for increasing PWLs compared with non-exposed rats (Fig. 3). Similar levels of PWLs were observed with rats exposed to 12, 36, or 110 lux GLED levels (Fig. 3). Exposure of rats to GLED 330 lux level significantly increased PWLs compared to baseline ambient-light exposed rats but resulted in only a half-maximal response when compared to the other lux conditions (Fig. 3). As the 4 lux GLED exposure for 8 hours was sufficient for achieving maximal antinociception, we used this lux level for all subsequent experiments.

We also tested if prolonged exposure to GLED could elicit tolerance to the antinociceptive effect. Rats exposed to GLED for an additional 7 days past the initial 5 days exposure (4 lux, 8 hr/day) – total of 12 days of GLED exposure – did not develop tolerance (Fig. 3B). This is in contrast to published data with morphine where analgesic tolerance can be observed within 3 days [67] and causes rats to be hyperalgesic within 5 days [82].

3.2. Characterization of the role of the visual system in the antinociceptive effects of GLED

We determined whether the mechanism of GLED-induced antinociception requires direct activation of the visual pathway by fashioning dark opaque plastic contact lenses that permitted no light penetration (confirmed by measuring light intensity). These were fitted onto the rats' eyes under anesthesia. As a control, transparent clear lenses were also installed

onto control rats's eyes. The application of contact lenses did not alter the baseline paw withdrawal latency. Both groups of rats were then exposed to GLED for eight hours daily for five days and their PWLs were monitored. Following this exposure paradigm, rats fitted with the dark, opaque contact lenses failed to develop antinociception, whereas rats fitted with clear, transparent contact lenses developed antinociception similar to rats with no contacts (Fig. 4A). Consistent with the importance of the visual system in the development of GLED-induced antinociception, rats fitted for eight hours with "green" contacts that permit light transmission in the green part of the visual spectrum (Fig. 4B), developed antinociception when exposed to room light (Fig. 4C). Importantly, histological analysis of the eyes of the rats at the end of the experiments revealed no damage caused by either contact lens (data not shown). These results support a role for the visual system in mediating the GLED mediated antinociception.

To test if pigmented skin is involved in the antinociceptive effects of GLED, we selected pigmented Long Evans (LE) rat, which are different from the albino Sprague-Dawley (SD) rats that lack pigmentation. A similar level of antinociception was observed in SD or LE rats exposed to GLED for eight hours daily for five days; the PWLs were significantly higher than the respective strains exposed to ambient light (Fig. 5). The antinociception was not restricted to male rats as female SD rats exposed to the same GLED paradigm also exhibited increased PWLs (Fig. 5). Collectively, these results suggest that pigmentation is not important for developing antinociception.

3.3. Pharmacological characterization of the antinociceptive effects of GLED

The mechanisms that might underlie the antinociceptive effects of GLED were investigated by determining possible contributions of endogenous pain transmitters and circuits as well as mediators of stress. Naïve rats exposed to GLED for eight hours daily for five days received antagonists immediately after light termination and then PWLs were measured 20–30 minutes later. The GLED-induced antinociception was reversed, to baseline levels, following a subcutaneous administration of the opioid receptor (MOR) antagonist naloxone (20 mg/kg i.p.). Twenty μg, intrathecal (i.t.) of naloxone also reversed the antinociception (Fig. 6A). These results suggest that GLED exposure likely elicits antinociception via release of endogenous opioids.

Neurons within the rostral ventromedial medulla (RVM) are known to project to the spinal or medullary dorsal horns to directly or indirectly enhance or diminish nociceptive traffic [85]. We examined the possible contribution of the RVM in the GLED-induced antinociceptive response by microinjection of 2% lidocaine. RVM lidocaine reversed the development of antinociception when the rats were exposed to GLED (Fig. 6B).

While our data thus far suggests a role for the endogenous opioid system, it is possible that the exposure conditions may result in stress-induced analgesia that could involve the sympathetic nervous system with engagement of alpha and beta-adrenergic receptors by nor-epinephrine or epinephrine [5; 10; 44; 50; 74; 78]. Thus, to elucidate the role of the adrenergic system, several adrenergic receptors antagonists were tested including phenoxybenzamine (1 mg/kg i.p), a nonselective irreversible alpha-blocker; phentolamine (3 mg/kg i.p), a nonselective reversible alpha-blocker; and propranolol (10 mg/kg s.c.), a

nonselective beta-blocker. All of these drugs given immediately after light termination and tested 15–20 minutes afterwards failed to prevent or reverse the antinociceptive effect of GLED (Fig. 7A). Additionally, rats exposed to GLED or ambient light were observed to have normal ambulation and huddling, as well as maintained regular grooming behaviors (data not shown), which is in contrast to diminished grooming observed in stressed rats [38].

To address the possibility of the antinociception being the result of anxiety due to overstimulation of the visual system, we performed elevated plus maze (EPM) experiments. A cohort of rats exposed to GLED for eight hours daily for five days developed antinociception as before (Fig. 7B), showed no signs of stress/anxiety as there were no differences in closed or open arm entries or in the anxiety index (Fig. 7C, D); the index combines EPM parameters into one unified ratio with values ranging from 0 to 1, with a higher value indicating increased anxiety [34]. In fact, rats exposed to GLED spent a significantly higher amount of time in the open arms than rats exposed to ambient room light (Fig. 7E), suggesting that GLED exposure was anxiolytic. Collectively, these results show that GLED-induced antinociception is not due to an anxiety related response in these rats.

3.4. Exposure to GLED does not impair motor performance

If, following exposure to GLED, the rats had a reduced motor activity, then this could contribute to the antinociception. To test this possibility, we investigated if the GLED exposure affected motor performance using the rotarod assay. Following verification of antinociceptive behaviors induced by exposure to GLED for eight hours daily for five days exhibited antinociception, we observed no change in the ability of the rats to stay on a rotating rod (Fig. 8). Thus, repeated GLED exposure does not affect motor performance or sedation.

3.5. Proteomics reveals GLED effects in the dorsal root ganglion and spinal dorsal horn

We used an unbiased-proteomics approach to identify possible protein alterations, using liquid chromatography-tandem mass spectrometry (LC-MS/MS), in tissues from ambient versus GLED exposed rats. Among 559 non-redundant protein identified in our DRG samples (Lumbar levels 4, 5 and 6 were pooled), 65 proteins were detected only in DRGs from GLED treated rats (Fig. 9A). Gene ontology (GO) terms corresponding to the biological processes (Fig. 9B), molecular functions (Fig. 9C), and cellular component (Fig. 9D) of these proteins identified in DRGs were extracted and compared between ambient and GLED exposed rats. We noted a higher number of proteins associated with the "response to stimulus" category and a fewer proteins associated with "growth" category in DRGs from GLED exposed rats compared to DRGs from ambient room light exposed rats (Fig. 9B). The molecular functions associated with these proteins suggests a decreased "structural molecule activity" and an increased "antioxidant activity" in DRGs from rats with GLED-induced thermal analgesia compared to controls (Fig. 9C). Finally, fewer proteins from GLED DRGs appear to be localized in "organelle part" and "membrane" (Fig. 9D).

A total of 430 non-redundant proteins were identified in dorsal horn tissues, of which 43 were found only in the samples from rats with GLED-induced thermal analgesia (Fig. 9E). We observed a higher number of proteins associated with "metabolic process" and "cellular

process" categories in dorsal horn from GLED exposed rats compared to dorsal horn from ambient room light exposed rats (Fig. 9F). The molecular functions associated with these proteins suggests a decreased "transporter activity" and an increased "binding" functions in dorsal horn from rats with GLED-induced thermal analgesia compared to controls (Fig. 9G). Finally, more proteins were observed to be in "cytoskeleton" and "intracellular organelles" while fewer proteins noted in "membrane", "plasma membrane" and "organelle membrane" in dorsal horn from GLED exposed rats compared to dorsal horn from ambient room light exposed rats (Fig. 9H). Thus, fewer proteins are localized in membranes in dorsal horn, which is correlated, with fewer proteins implicated in localization processes in DRGs.

3.6. Analgesic effects of GLED exposure in neuropathic pain

Having determined that GLED is antinociceptive in naïve animals, we next asked if this non-pharmacological paradigm could be effective in reversing allodynia and hyperalgesia associated with the SNL model of experimental neuropathic pain. Probing the plantar surface of the hindpaw ipsilateral to the side of nerve injury in SNL rats, 7 days post injury, revealed thermal hyperalgesia (Fig. 10A) and tactile allodynia (Fig. 10B). Exposing SNL-injured rats for eight hours daily to 4 lux GLED levels resulted in complete reversal of thermal hyperalgesia; the latencies were significantly higher than baseline so as to be antinociceptive (Fig. 10A). Paw withdrawal thresholds were also maximally reversed by a 3 day exposure to GLED (Fig. 10B). To address the duration of the GLED effect in SNL rats, we terminated GLED exposure and continued to measure anti-hyperalgesic and antiallodynic behaviors. After termination of GLED, it took ten days for the thermal latencies (Fig. 10C) and four days for mechanical thresholds to return to post-surgical values (Fig. 10D).

Using qRT-PCR, we determined expression levels of mRNAs for various endogenous opioids in spinal cords of naïve rats as well as rats with SNL or sham in the presence of GLED exposure. Expression of the following genes was measured: (*i*) Prepronociceptin (PNOC) coding for Nocistatin, Nociceptin, and Orphanin FQ2 [17]; (*ii*) Pro-opiomelanocortin (POMC) coding for NPP, Melanotropin gamma, corticotropin, melanotropin alpha, Lipotropin beta, Lipotropin gamma, Melanotropin beta, Beta-endorphin and Met-enkephalin [11]; (*iii*) Proenkephalin-A (PENK) coding for Synenkephalin, Met-enkephalin (4 copies), Met-enkephalin-Arg-Gly-Leu, Met-enkephalin-Arg-Phe and Leu-enkephalin [18]; (*iv*) Proenkephalin-B (PDYN) coding for Alpha-neoendorphin, Beta-neoendorphin, and Leu-enkephalin (3 copies), Big dynorphin, Dynorphin A(1–17), Dynorphin A(1–13), Dynorphin A(1–8), Leumorphin and Rimorphin [17]; and (*v*) Mu-type opioid receptor (OPRM1) coding for preproniceptin and Pro-opiomelanocortin [60]. These analyses demonstrate that expression of PENK gene, but not others, is significantly increased after GLED exposure (Fig. 10E), suggesting that the increased enkephalin levels in the spinal cord of green LED exposed rats could be one contributing factor for their analgesia.

4. Discussion

We characterized the antinociceptive and anti-hyperalgesic effects of GLED phototherapy. In naïve rats, the antinociceptive effect of GLED involves (1) visual system, (2) mu-opioid receptor pathways and descending pain inhibitory pathways from the RVM, (3) increased spinal cord expression of enkephalins, and (4) alterations in spinal cord and nociceptor proteomes. We were unable to link GLED-mediated antinociception to stress/anxiety. We demonstrate GLED phototherapy's ability to reverse reduced sensory thresholds in a model of neuropathic pain, supporting its use as a possible novel, non-pharmacological approach in managing chronic pain.

A key issue in interpreting photically-induced antinociception is delineating the route of entry of light and its possible relationship to pain modulatory circuits. Here, whole body illumination with GLED for eight hours resulted in antinociception. In contrast, previous studies reported reversal of pain in mice following 30–150 seconds of infrared LED exposure directly touching the skin [15; 16]. The differences in exposure times (seconds versus hours) and "routes of administration" with either direct skin exposure or whole body illumination could result in engagement of different mechanisms. Additionally, lower intensity GLED was more antinociceptive. These results are consistent with a recent study [62], which reported that low intensity green light reduced the intensity of migraines by ~15% compared to lights of other colors and higher intensities.

Blocking GLED access to the eyes prevented antinociception, arguing for an important role by the visual system in the development of antinociception. Our data point to a role for the visual system in the antinociceptive and antiallodynic effects of GLED. However, exactly how this occurs is unknown. Electrical stimulation of the optic nerves in rats has been reported to increase blood pressure and heart rate, and to decrease baroreceptor mediated vagal bradycardia. This effect was largely attenuated by inactivation of the periaqueductal grey (PAG), an anatomical region known to modulate pain [33; 53], suggesting mechanistic neural links between the optic nerve and the PAG [13]. Light sensitive melanopsin-containing ganglion cells in the eyes [68] project directly to the circadian rhythm controlling suprachiasmatic nucleus (SCN) [31; 80] and PAG [30]; these structures are connected [41]. Importantly, the SCN has been linked to pain as inferred from disruption of the circadian rhythm of thermoregulation in models of chronic inflammatory pain in rats [75] and increased c-Fos levels in rat with cystitis pain [6]. Finally, a retrograde labeling of the PAG demonstrated glutamate-like immunoreactivity in several regions of the brain including the occipital cortices [4], further supporting a link between the visual system and pain response. Martenson and colleagues [51] have recently identified a possible circuitry for photic stimulation that included pain modulating "ON-cells" and "OFF-cells" in the RVM which project to the dorsal horn of the spinal cord where they are postulated to modulate somatosensory processing. An imbalance of these may lead to enhanced or diminished pain with ON-cells facilitating nociception and OFF-cells inhibiting nociception. Our studies support a role for the RVM as its chemical inactivation prevented GLED-induced antinociception.

We demonstrated GLED-induced antinociception involves opioid receptors. However, whether this occurs via a peripheral or central mechanism of action is at present unknown. Suppression of GLED-induced antinociception with the opioid receptor antagonist naloxone, administered systemically, may support a role of peripheral opioid receptors, which is consistent with previous reports demonstrating that administration of naloxone prevents infrared spectrum therapy induced antinociception in models of post-operative [16] or inflammatory pain [52]. However, the ability of naloxone given intrathecally to reverse the antinociception effect argues in favor of a central site of action for the GLED since this dose and volume would not be expected to have a significant effect if the site of action was in the periphery. It is conceivable that GLED may have both central and peripheral effects. Future studies will explore these possibilities.

While overstimulation of the visual system could cause stress-induced antinociception, our data suggest GLED-induced antinociception is not linked to stress/anxiety for several reasons. First, pharmacological antagonism of receptors implicated in stress did not affect antinociception. Second, behavioral studies did not link GLED-induced antinociception to anxiety in the elevated plus maze experiments. Finally, grooming behaviors of rats with GLED exposures were unaffected implying no link to stress. Future studies will assess neurochemical correlates of stress (e.g., glucocorticoids) in GLED antinociception.

Sensory neuronal adaptations, due to possible changes in activities of voltage-gated calcium and/or sodium channels, may help explain the molecular mechanisms underlying GLED-induced antinociception. N-type voltage-gated calcium channels (CaV2.2) are key for antinociception [73]. The overall functional competence of neurons for calcium influx, as assessed by their ability to respond to agonists of various receptors using a high-throughput calcium imaging platform [55], was not different between sensory neurons from rats exposed to ambient light or GLED (Supplementary Figure 1). However, we observed a decrease in depolarization-induced Ca^{2+} influx via CaV2.2 in sensory neurons from GLED exposed rats (Supplementary Figure 1E). No changes were observed in sodium channels (Supplementary Figure 2) ruling out their involvement in neuronal adaptations and GLED-induced analgesia. It is possible that the prolonged antinociceptive effect of GLED may, in part, be attributed to long-term changes in CaV2.2 or other calcium channel subtypes. Further studies will investigate the role of calcium and other channels in mediating the long-lasting effect of GLED.

Unbiased proteomics identified a protein signature in dorsal root ganglia and dorsal horn of GLED-exposed antinociceptive rats. Stratification of proteins based on gene ontology (GO) terms corresponding to biological processes, molecular functions, and cellular components revealed an enrichment of proteins related to "antioxidant activity" in ganglia of GLED-exposed rats, a finding consistent with reported reduction in antioxidant activities (e.g., catalase and superoxide dismutase) in rats with inflammatory pain [52]. Additionally, low-level light therapy reduces levels of inflammatory mediators (e.g., interleukins 6 and 8) associated with intervertebral disc degeneration, a key cause of low back pain [35]. We noted a reduction in the number of membrane-localized proteins in dorsal horn of GLED-exposed rats, which likely correlates with decreased signaling capabilities of neurons. Our findings uncovered proteins enriched in tissues from GLED exposed rats that are reportedly

linked to antinociception (Table 3). For example, purine nucleoside phosphorylase breaks down adenosine into inosine, which has antinociceptive properties via actions on the Adenosine A1 receptor [57] and via pertussis toxin-sensitive G-protein coupled receptors and the subsequent inactivation of calcium channels [49]. Aspartyl aminopeptidase, which converts angiotensin II to angiotensin III, is reported to activate inhibitory pain descending pathways from the PAG [65]. Our findings of chemical inactivation of the RVM further support a role of inhibitory pain descending pathways in GLED mediated antinociception. Another example is lactoylglutathione lyase (i.e., glyoxalase-1), which catalyzes the detoxification of methylglyoxal, a cytotoxic ketoaldehyde, which is directly linked to activating nociceptors [1]. Moreover, expression of glyoxalase-1 is reduced in diabetic neuropathy [37]. These lines of evidence, along with those listed in Table 3, build a picture consistent with global changes induced by GLED to produce antinociception.

We used a model of neuropathic pain to illustrate the possible use of GLED as a non-pharmacological treatment. Spinal nerve ligation (SNL) is a commonly used model of neuropathic pain in rats [40]. Common neuropathic pain medications reverse hypersensitivity associated with neuropathic conditions, but do not usually produce antinociception. For example, gabapentin blocks the N-type calcium channel [47] to reverse tactile allodynia and thermal hyperalgesia in diabetic neuropathy, however, it failed to produce antinociception [69]. Carbamazepine, an antiepileptic medication used for neuropathic pain, blocks sodium channels to reverse thermal hyperalgesia in tail flick test in a model of cis-platin induced hyperalgesia, but fails to produce antinociception [54]. In contrast, GLED reversed tactile and thermal hypersensitivity associated with SNL and produced long-lasting antinociception. We observed that GLED decreased calcium influx via the N-type calcium channel (supplementary Figure 1F), which may account for both the anti-allodynic and -hyperalgesic effects; however, the exact mechanisms contributing to the long-lasting nature of the effect is presently unknown. We also observed that GLED activates opioid receptors, which may account for antiallodynia, antihyperalgesia and antinociception. The complete reversal of the effects of GLED using naloxone also argues for a key role for opioid receptors in producing antiallodynia, antihyperalgesia and antinociception. It is conceivable that multiple mechanisms of actions may act synergistically to produce the effects seen with GLED. In contrast to the side-effects observed with opioids, an advantage of the GLED approach is lack of side effects such as development of tolerance, sedation, respiratory depression, and motor coordination. Equally important was the lack of hyperalgesia following prolonged GLED exposure. The lack of these side effects suggests that using GLED may be a safe treatment for neuropathic, and other pain states, and may also complement the use of pain medications.

Our findings identify cellular and molecular basis of GLED–mediated antinociception. From a translational perspective, the discovery that GLED exposure is antinociceptive and antiallodynic, opens up routes for the development of a non-invasive therapeutic approach for pain. Consequently, modulating the duration and intensity of GLED may prove useful clinically for reducing opioid for pain management. Additionally, the long-lasting and non-tolerance inducing effects of GLED may improve patient compliance.

Supplementary Material

Refer to Web version on PubMed Central for supplementary material.

Acknowledgments

References

1. Andersson DA, Gentry C, Light E, Vastani N, Vallortigara J, Bierhaus A, Fleming T, Bevan S. Methylglyoxal evokes pain by stimulating TRPA1. PloS one. 2013; 8(10):e77986. [PubMed: 24167592]

2. Andre J, Zeau B, Pohl M, Cesselin F, Benoliel JJ, Becker C. Involvement of cholecystokininergic systems in anxiety-induced hyperalgesia in male rats: behavioral and biochemical studies. J Neurosci. 2005; 25(35):7896–7904. [PubMed: 16135746]

3. Ashburner M, Ball CA, Blake JA, Botstein D, Butler H, Cherry JM, Davis AP, Dolinski K, Dwight SS, Eppig JT, Harris MA, Hill DP, Issel-Tarver L, Kasarskis A, Lewis S, Matese JC, Richardson JE, Ringwald M, Rubin GM, Sherlock G. Gene ontology: tool for the unification of biology. The Gene Ontology Consortium. Nat Genet. 2000; 25(1):25–29. [PubMed: 10802651]

4. Beitz AJ. Possible origin of glutamatergic projections to the midbrain periaqueductal gray and deep layer of the superior colliculus of the rat. Brain research bulletin. 1989; 23(1–2):25–35. [PubMed: 2478264]

5. Bodnar RJ, Kelly DD, Brutus M, Greenman CB, Glusman M. Reversal of stress-induced analgesia by apomorphine, but not by amphetamine. Pharmacol Biochem Behav. 1980; 13(2):171–175. [PubMed: 7413686]

6. Bon K, Lanteri-Minet M, de Pommery J, Michiels JF, Menetrey D. Cyclophosphamide cystitis as a model of visceral pain in rats: minor effects at mesodiencephalic levels as revealed by the expression of c-fos, with a note on Krox-24. Experimental brain research. 1997; 113(2):249–264. [PubMed: 9063711]

7. Bonafe L, Kariminejad A, Li J, Royer-Bertrand B, Garcia V, Mahdavi S, Bozorgmehr B, Lachman RL, Mittaz-Crettol L, Campos-Xavier B, Nampoothiri S, Unger S, Rivolta C, Levade T, Superti-Furga A. Peripheral osteolysis in adults linked to ASAH1 (acid ceramidase) mutations: A new presentation of Farber disease. Arthritis Rheumatol. 2016

8. Brittain JM, Piekarz AD, Wang Y, Kondo T, Cummins TR, Khanna R. An atypical role for collapsin response mediator protein 2 (CRMP-2) in neurotransmitter release via interaction with presynaptic voltage-gated calcium channels. The Journal of biological chemistry. 2009; 284(45):31375–31390. [PubMed: 19755421]

9. Bushnell MC, Ceko M, Low LA. Cognitive and emotional control of pain and its disruption in chronic pain. Nature reviews Neuroscience. 2013; 14(7):502–511. [PubMed: 23719569]

10. Butler RK, Finn DP. Stress-induced analgesia. Prog Neurobiol. 2009; 88(3):184–202. [PubMed: 19393288]

11. Cakir I, Cyr NE, Perello M, Litvinov BP, Romero A, Stuart RC, Nillni EA. Obesity induces hypothalamic endoplasmic reticulum stress and impairs proopiomelanocortin (POMC) post-translational processing. The Journal of biological chemistry. 2013; 288(24):17675–17688. [PubMed: 23640886]

12. Chaplan SR, Bach FW, Pogrel JW, Chung JM, Yaksh TL. Quantitative assessment of tactile allodynia in the rat paw. Journal of neuroscience methods. 1994; 53(1):55–63. [PubMed: 7990513]

13. Cheng ZB, Kobayashi M, Nosaka S. Effects of optic tract stimulation on baroreflex vagal bradycardia in rats. Clinical and experimental pharmacology & physiology. 2001; 28(9):721–728. [PubMed: 11553030]

14. Chipkin RE, Latranyi MZ, Iorio LC, Barnett A. Potentiation of [D-ala2]enkephalinamide analgesia in rats by thiorphan. European journal of pharmacology. 1982; 83(3–4):283–288. [PubMed: 6756941]

15. Cidral-Filho FJ, Martins DF, More AO, Mazzardo-Martins L, Silva MD, Cargnin-Ferreira E, Santos AR. Light-emitting diode therapy induces analgesia and decreases spinal cord and sciatic nerve tumour necrosis factor-alpha levels after sciatic nerve crush in mice. Eur J Pain. 2013; 17(8): 1193–1204. [PubMed: 23339021]

16. Cidral-Filho FJ, Mazzardo-Martins L, Martins DF, Santos AR. Light-emitting diode therapy induces analgesia in a mouse model of postoperative pain through activation of peripheral opioid receptors and the L-arginine/nitric oxide pathway. Lasers Med Sci. 2014; 29(2):695–702. [PubMed: 23832179]

17. D'Addario C, Caputi FF, Ekstrom TJ, Di Benedetto M, Maccarrone M, Romualdi P, Candeletti S. Ethanol induces epigenetic modulation of prodynorphin and pronociceptin gene expression in the rat amygdala complex. J Mol Neurosci. 2013; 49(2):312–319. [PubMed: 22684622]

18. Denning GM, Ackermann LW, Barna TJ, Armstrong JG, Stoll LL, Weintraub NL, Dickson EW. Proenkephalin expression and enkephalin release are widely observed in non-neuronal tissues. Peptides. 2008; 29(1):83–92. [PubMed: 18082911]

19. Dworkin RH, O'Connor AB, Backonja M, Farrar JT, Finnerup NB, Jensen TS, Kalso EA, Loeser JD, Miaskowski C, Nurmikko TJ, Portenoy RK, Rice AS, Stacey BR, Treede RD, Turk DC, Wallace MS. Pharmacologic management of neuropathic pain: evidence-based recommendations. Pain. 2007; 132(3):237–251. [PubMed: 17920770]

20. Eastman CI, Young MA, Fogg LF, Liu L, Meaden PM. Bright light treatment of winter depression: a placebo-controlled trial. Archives of general psychiatry. 1998; 55(10):883–889. [PubMed: 9783558]

21. Figueiro MG, Plitnick BA, Lok A, Jones GE, Higgins P, Hornick TR, Rea MS. Tailored lighting intervention improves measures of sleep, depression, and agitation in persons with Alzheimer's disease and related dementia living in long-term care facilities. Clinical interventions in aging. 2014; 9:1527–1537. [PubMed: 25246779]

22. Finnerup NB, Attal N, Haroutounian S, McNicol E, Baron R, Dworkin RH, Gilron I, Haanpaa M, Hansson P, Jensen TS, Kamerman PR, Lund K, Moore A, Raja SN, Rice AS, Rowbotham M, Sena E, Siddall P, Smith BH, Wallace M. Pharmacotherapy for neuropathic pain in adults: a systematic review and meta-analysis. Lancet neurology. 2015; 14(2):162–173. [PubMed: 25575710]

23. Fricova J, Vejrazka M, Stopka P, Krizova J, Belacek J, Rokyta R. The influence of pre-emptive analgesia on postoperative analgesia and its objective evaluation. Arch Med Sci. 2010; 6(5):764–771. [PubMed: 22419937]

24. Gaskin ME, Greene AF, Robinson ME, Geisser ME. Negative affect and the experience of chronic pain. J Psychosom Res. 1992; 36(8):707–713. [PubMed: 1432860]

25. Golden RN, Gaynes BN, Ekstrom RD, Hamer RM, Jacobsen FM, Suppes T, Wisner KL, Nemeroff CB. The efficacy of light therapy in the treatment of mood disorders: a review and meta-analysis of the evidence. The American journal of psychiatry. 2005; 162(4):656–662. [PubMed: 15800134]

26. Gray D, Coon H, McGlade E, Callor WB, Byrd J, Viskochil J, Bakian A, Yurgelun-Todd D, Grey T, McMahon WM. Comparative analysis of suicide, accidental, and undetermined cause of death classification. Suicide & life-threatening behavior. 2014; 44(3):304–316. [PubMed: 25057525]

27. Gungor D, Schober AK, Kruijshaar ME, Plug I, Karabul N, Deschauer M, van Doorn PA, van der Ploeg AT, Schoser B, Hanisch F. Pain in adult patients with Pompe disease: a cross-sectional survey. Mol Genet Metab. 2013; 109(4):371–376. [PubMed: 23849261]

28. Hargreaves K, Dubner R, Brown F, Flores C, Joris J. A new and sensitive method for measuring thermal nociception in cutaneous hyperalgesia. Pain. 1988; 32(1):77–88. [PubMed: 3340425]

29. Hassett AL, Aquino JK, Ilgen MA. The risk of suicide mortality in chronic pain patients. Current pain and headache reports. 2014; 18(8):436. [PubMed: 24952608]

30. Hattar S, Kumar M, Park A, Tong P, Tung J, Yau KW, Berson DM. Central projections of melanopsin-expressing retinal ganglion cells in the mouse. The Journal of comparative neurology. 2006; 497(3):326–349. [PubMed: 16736474]

31. Hattar S, Liao HW, Takao M, Berson DM, Yau KW. Melanopsin-containing retinal ganglion cells: architecture, projections, and intrinsic photosensitivity. Science. 2002; 295(5557):1065–1070. [PubMed: 11834834]

32. Hooley JM, Franklin JC, Nock MK. Chronic pain and suicide: understanding the association. Current pain and headache reports. 2014; 18(8):435. [PubMed: 24916035]

33. Hosobuchi Y. Combined electrical stimulation of the periaqueductal gray matter and sensory thalamus. Appl Neurophysiol. 1983; 46(1–4):112–115. [PubMed: 6608316]

34. Huynh TN, Krigbaum AM, Hanna JJ, Conrad CD. Sex differences and phase of light cycle modify chronic stress effects on anxiety and depressive-like behavior. Behavioural brain research. 2011; 222(1):212–222. [PubMed: 21440009]

35. Hwang MH, Shin JH, Kim KS, Yoo CM, Jo GE, Kim JH, Choi H. Low Level Light Therapy Modulates Inflammatory Mediators Secreted by Human Annulus Fibrosus Cells during Intervertebral Disc Degeneration In Vitro. Photochemistry and photobiology. 2015; 91(2):403–410. [PubMed: 25557915]

36. Institute of Medicine (U.S.). Committee on Advancing Pain Research Care and Education. Relieving pain in America : a blueprint for transforming prevention, care, education, and research. Washington, D.C.: National Academies Press; 2011.

37. Jack MM, Ryals JM, Wright DE. Protection from diabetes-induced peripheral sensory neuropathy–a role for elevated glyoxalase I? Experimental neurology. 2012; 234(1):62–69. [PubMed: 22201551]

38. Katz RJ, Roth KA. Stress induced grooming in the rat–an endorphin mediated syndrome. Neuroscience letters. 1979; 13(2):209–212. [PubMed: 530471]

39. Kim DS, Lee SJ, Park SY, Yoo HJ, Kim SH, Kim KJ, Cho HJ. Differentially expressed genes in rat dorsal root ganglia following peripheral nerve injury. Neuroreport. 2001; 12(15):3401–3405. [PubMed: 11711894]

40. Kim KJ, Yoon YW, Chung JM. Comparison of three rodent neuropathic pain models. Experimental brain research Experimentelle Hirnforschung Experimentation cerebrale. 1997; 113(2):200–206. [PubMed: 9063706]

41. Krout KE, Kawano J, Mettenleiter TC, Loewy AD. CNS inputs to the suprachiasmatic nucleus of the rat. Neuroscience. 2002; 110(1):73–92. [PubMed: 11882374]

42. Lambert D'raven LT, Moliver N, Thompson D. Happiness intervention decreases pain and depression, boosts happiness among primary care patients. Primary health care research & development. 2015; 16(2):114–126. [PubMed: 24451155]

43. Leichtfried V, Matteucci Gothe R, Kantner-Rumplmair W, Mair-Raggautz M, Bartenbach C, Guggenbichler H, Gehmacher D, Jonas L, Aigner M, Winkler D, Schobersberger W. Short-term effects of bright light therapy in adults with chronic nonspecific back pain: a randomized controlled trial. Pain medicine. 2014; 15(12):2003–2012. [PubMed: 25159085]

44. Lewis JW, Cannon JT, Liebeskind JC. Opioid and nonopioid mechanisms of stress analgesia. Science. 1980; 208(4444):623–625. [PubMed: 7367889]

45. Li Y, Hu F, Chen HJ, Du YJ, Xie ZY, Zhang Y, Wang J, Wang Y. LIMK-dependent actin polymerization in primary sensory neurons promotes the development of inflammatory heat hyperalgesia in rats. Sci Signal. 2014; 7(331):ra61. [PubMed: 24962708]

46. Linton SJ, Shaw WS. Impact of psychological factors in the experience of pain. Phys Ther. 2011; 91(5):700–711. [PubMed: 21451097]

47. Liukkonen A. The nurse's decision-making process and the implementation of psychogeriatric nursing in a mental hospital. J Adv Nurs. 1992; 17(3):356–361. [PubMed: 1573104]

48. Livak KJ, Schmittgen TD. Analysis of relative gene expression data using real-time quantitative PCR and the 2(-Delta Delta C(T)) Method. Methods. 2001; 25(4):402–408. [PubMed: 11846609]

49. Macedo-Junior SJ, Nascimento FP, Luiz-Cerutti M, Santos AR. Role of pertussis toxin-sensitive G-protein, K+ channels, and voltage-gated Ca2+ channels in the antinociceptive effect of inosine. Purinergic Signal. 2013; 9(1):51–58. [PubMed: 22806273]

50. Maier SF. Stressor controllability and stress-induced analgesia. Ann N Y Acad Sci. 1986; 467:55–72. [PubMed: 3524388]

51. Martenson ME, Halawa OI, Tonsfeldt KJ, Maxwell CA, Hammack N, Mist SD, Pennesi ME, Bennett RM, Mauer KM, Jones KD, Heinricher MM. A possible neural mechanism for photosensitivity in chronic pain. Pain. 2016; 157(4):868–878. [PubMed: 26785323]

52. Martins DF, Turnes BL, Cidral-Filho FJ, Bobinski F, Rosas RF, Danielski LG, Petronilho F, Santos AR. Light-emitting diode therapy reduces persistent inflammatory pain: Role of interleukin 10 and antioxidant enzymes. Neuroscience. 2016; 324:485–495. [PubMed: 27001179]

53. Millan MJ. Descending control of pain. Prog Neurobiol. 2002; 66(6):355–474. [PubMed: 12034378]

54. Mohajjel Nayebi A, Sharifi H, Ramadzani M, Rezazadeh H. Effect of acute and chronic administration of carbamazepine on Cisplatin-induced hyperalgesia in rats. Jundishapur J Nat Pharm Prod. 2012; 7(1):27–30. [PubMed: 24624148]

55. Moutal A, Chew LA, Yang X, Wang Y, Yeon SK, Telemi E, Meroueh S, Park KD, Shrinivasan R, Gilbraith KB, Qu C, Xie JY, Patwardhan A, Vanderah TW, Khanna M, Porreca F, Khanna R. (S)-Lacosamide inhibition of CRMP2 phosphorylation reduces postoperative and neuropathic pain behaviors through distinct classes of sensory neurons identified by constellation pharmacology. Pain. 2016

56. Moutal A, Honnorat J, Massoma P, Desormeaux P, Bertrand C, Malleval C, Watrin C, Chounlamountri N, Mayeur ME, Besancon R, Naudet N, Magadoux L, Khanna R, Ducray F, Meyronet D, Thomasset N. CRMP5 Controls Glioblastoma Cell Proliferation and Survival through Notch-Dependent Signaling. Cancer Res. 2015; 75(17):3519–3528. [PubMed: 26122847]

57. Nascimento FP, Macedo-Junior SJ, Pamplona FA, Luiz-Cerutti M, Cordova MM, Constantino L, Tasca CI, Dutra RC, Calixto JB, Reid A, Sawynok J, Santos AR. Adenosine A1 receptor-dependent antinociception induced by inosine in mice: pharmacological, genetic and biochemical aspects. Mol Neurobiol. 2015; 51(3):1368–1378. [PubMed: 25064055]

58. Navratilova E, Xie JY, King T, Porreca F. Evaluation of reward from pain relief. Annals of the New York Academy of Sciences. 2013; 1282(1):1–11. [PubMed: 23496247]

59. Nesvizhskii AI, Keller A, Kolker E, Aebersold R. A statistical model for identifying proteins by tandem mass spectrometry. Anal Chem. 2003; 75(17):4646–4658. [PubMed: 14632076]

60. Ni J, Gao Y, Gong S, Guo S, Hisamitsu T, Jiang X. Regulation of mu-opioid type 1 receptors by microRNA134 in dorsal root ganglion neurons following peripheral inflammation. Eur J Pain. 2013; 17(3):313–323. [PubMed: 22865422]

61. Niederhofer H, von Klitzing K. Bright light treatment as add-on therapy for depression in 28 adolescents: a randomized trial. Prim Care Companion CNS Disord. 2011; 13(6)

62. Noseda R, Bernstein CA, Nir RR, Lee AJ, Fulton AB, Bertisch SM, Hovaguimian A, Cestari DM, Saavedra-Walker R, Borsook D, Doran BL, Buettner C, Burstein R. Migraine photophobia originating in cone-driven retinal pathways. Brain : a journal of neurology. 2016

63. Nyberg MA, Peyman GA, McEnerney JK. Evaluation of donor corneal endothelial viability with the vital stains rose bengal and evans blue. Albrecht Von Graefes Arch Klin Exp Ophthalmol. 1977; 204(3):153–159. [PubMed: 74214]

64. Pecze L, Blum W, Schwaller B. Mechanism of capsaicin receptor TRPV1-mediated toxicity in pain-sensing neurons focusing on the effects of $Na(+)/Ca(2+)$ fluxes and the $Ca(2+)$-binding protein calretinin. Biochimica et biophysica acta. 2013; 1833(7):1680–1691. [PubMed: 22982061]

65. Pelegrini-da-Silva A, Rosa E, Guethe LM, Juliano MA, Prado WA, Martins AR. Angiotensin III modulates the nociceptive control mediated by the periaqueductal gray matter. Neuroscience. 2009; 164(3):1263–1273. [PubMed: 19747525]

66. Pihl TH, Andersen PH, Kjelgaard-Hansen M, Morck NB, Jacobsen S. Serum amyloid A and haptoglobin concentrations in serum and peritoneal fluid of healthy horses and horses with acute abdominal pain. Vet Clin Pathol. 2013; 42(2):177–183. [PubMed: 23577834]

67. Porreca F, Cowan A, Raffa RB, Tallarida RJ. Tolerance and cross-tolerance studies with morphine and ethylketocyclazocine. The Journal of pharmacy and pharmacology. 1982; 34(10):666–667. [PubMed: 6128391]

68. Provencio I, Rodriguez IR, Jiang G, Hayes WP, Moreira EF, Rollag MD. A novel human opsin in the inner retina. The Journal of neuroscience : the official journal of the Society for Neuroscience. 2000; 20(2):600–605. [PubMed: 10632589]

69. Reda HM, Zaitone SA, Moustafa YM. Effect of levetiracetam versus gabapentin on peripheral neuropathy and sciatic degeneration in streptozotocin-diabetic mice: Influence on spinal microglia and astrocytes. Eur J Pharmacol. 2016; 771:162–172. [PubMed: 26712375]

70. Shah K, Lahiri DK. A Tale of the Good and Bad: Remodeling of the Microtubule Network in the Brain by Cdk5. Mol Neurobiol. 2016

71. Levinson DM, Sheridan CL, Hottman TJ, Justesen DR, Creel DJ, Sanders RE. Assessment of the contact eye cover as an effective method of restricting visual input. Bahavior Research Methods & Instrumentation. 1978; 10(3):376–388.

72. Smith AA, Friedemann ML. Perceived family dynamics of persons with chronic pain. Journal of advanced nursing. 1999; 30(3):543–551. [PubMed: 10499210]

73. Snutch TP. Targeting chronic and neuropathic pain: the N-type calcium channel comes of age. NeuroRx. 2005; 2(4):662–670. [PubMed: 16489373]

74. Spradley JM, Davoodi A, Carstens MI, Carstens E. Effects of acute stressors on itch- and pain-related behaviors in rats. Pain. 2012; 153(9):1890–1897. [PubMed: 22770638]

75. Stein C, Millan MJ, Herz A. Unilateral inflammation of the hindpaw in rats as a model of prolonged noxious stimulation: alterations in behavior and nociceptive thresholds. Pharmacology, biochemistry, and behavior. 1988; 31(2):445–451.

76. Strigo IA, Simmons AN, Matthews SC, Craig AD, Paulus MP. Association of major depressive disorder with altered functional brain response during anticipation and processing of heat pain. Arch Gen Psychiatry. 2008; 65(11):1275–1284. [PubMed: 18981339]

77. Sun L, Wu Z, Hayashi Y, Peters C, Tsuda M, Inoue K, Nakanishi H. Microglial cathepsin B contributes to the initiation of peripheral inflammation-induced chronic pain. The Journal of neuroscience : the official journal of the Society for Neuroscience. 2012; 32(33):11330–11342. [PubMed: 22895716]

78. Takahashi M, Izumi R, Kaneto H. The role of the catecholaminergic mechanism in foot shock (FS) stress- and immobilized-water immersion (IW) stress-induced analgesia in mice. Jpn J Pharmacol. 1984; 35(2):175–179. [PubMed: 6540323]

79. Tse MM, Lo AP, Cheng TL, Chan EK, Chan AH, Chung HS. Humor therapy: relieving chronic pain and enhancing happiness for older adults. Journal of aging research. 2010; 2010:343574. [PubMed: 21151506]

80. van Esseveldt KE, Lehman MN, Boer GJ. The suprachiasmatic nucleus and the circadian time-keeping system revisited. Brain research Brain research reviews. 2000; 33(1):34–77. [PubMed: 10967353]

81. Vivacqua G, Yin JJ, Casini A, Li X, Li YH, D'Este L, Chan P, Renda TG, Yu S. Immunolocalization of alpha-synuclein in the rat spinal cord by two novel monoclonal antibodies. Neuroscience. 2009; 158(4):1478–1487. [PubMed: 19118601]

82. Xie JY, Herman DS, Stiller CO, Gardell LR, Ossipov MH, Lai J, Porreca F, Vanderah TW. Cholecystokinin in the rostral ventromedial medulla mediates opioid-induced hyperalgesia and antinociceptive tolerance. The Journal of neuroscience : the official journal of the Society for Neuroscience. 2005; 25(2):409–416. [PubMed: 15647484]

83. Yaksh TL, Rudy TA. Chronic catheterization of the spinal subarachnoid space. Physiology & behavior. 1976; 17(6):1031–1036. [PubMed: 14677603]

84. Zhan J, Chen X, Wang C, Qiu J, Ma F, Wang K, Zheng S. A fusion protein of conotoxin MVIIA and thioredoxin expressed in Escherichia coli has significant analgesic activity. Biochemical and biophysical research communications. 2003; 311(2):495–500. [PubMed: 14592443]

85. Zhang Y, Zhao S, Rodriguez E, Takatoh J, Han BX, Zhou X, Wang F. Identifying local and descending inputs for primary sensory neurons. The Journal of clinical investigation. 2015; 125(10):3782–3794. [PubMed: 26426077]

86. Zhou J, Tawk M, Tiziano FD, Veillet J, Bayes M, Nolent F, Garcia V, Servidei S, Bertini E, Castro-Giner F, Renda Y, Carpentier S, Andrieu-Abadie N, Gut I, Levade T, Topaloglu H, Melki J. Spinal muscular atrophy associated with progressive myoclonic epilepsy is caused by mutations in ASAH1. Am J Hum Genet. 2012; 91(1):5–14. [PubMed: 22703880]

87. Zulauf L, Coste O, Marian C, Moser C, Brenneis C, Niederberger E. Cofilin phosphorylation is involved in nitric oxide/cGMP-mediated nociception. Biochemical and biophysical research communications. 2009; 390(4):1408–1413. [PubMed: 19896457]
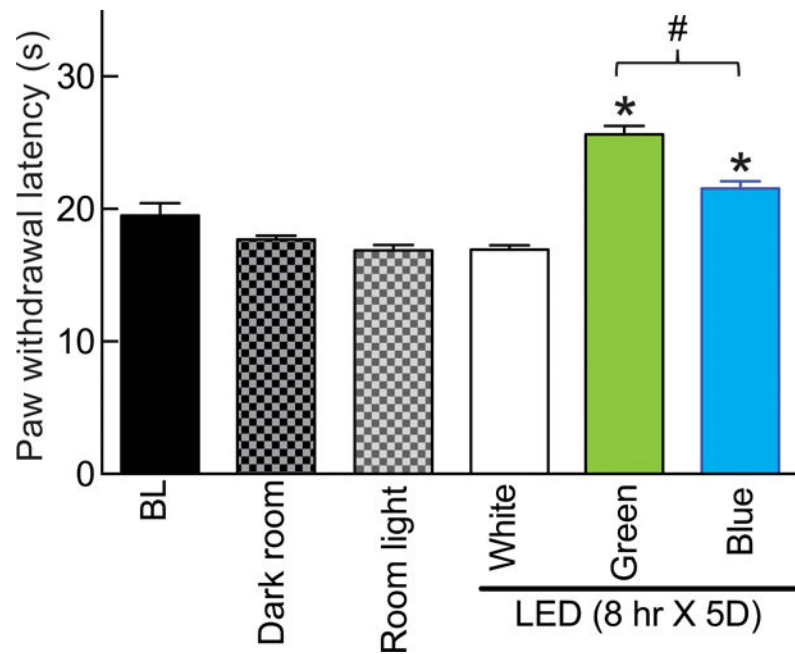
Figure 1. Effect of light emitting diode (LED) exposure on thermal analgesia in naïve rats

Following measurement of baseline (BL) paw withdrawal latency (PWL, seconds), rats were randomly assigned (n=6 per group) to exposures of eight hours daily for five days to: dark; ambient room light; or white, green (λ=525 nm) or blue (λ=472 nm) LED. At the end of this exposure paradigm, PWLs were again measured. Blue and GLED exposure resulted in thermal analgesia. *p<0.05 when comparing to white LED (one-way ANOVA followed by Student-Newman-Keuls test) and #p<0.05 when comparing between green and blue LED exposures (non-parametric Student's t-test). Unless otherwise stated, the data represent mean ± SEM for all figures in this manuscript.
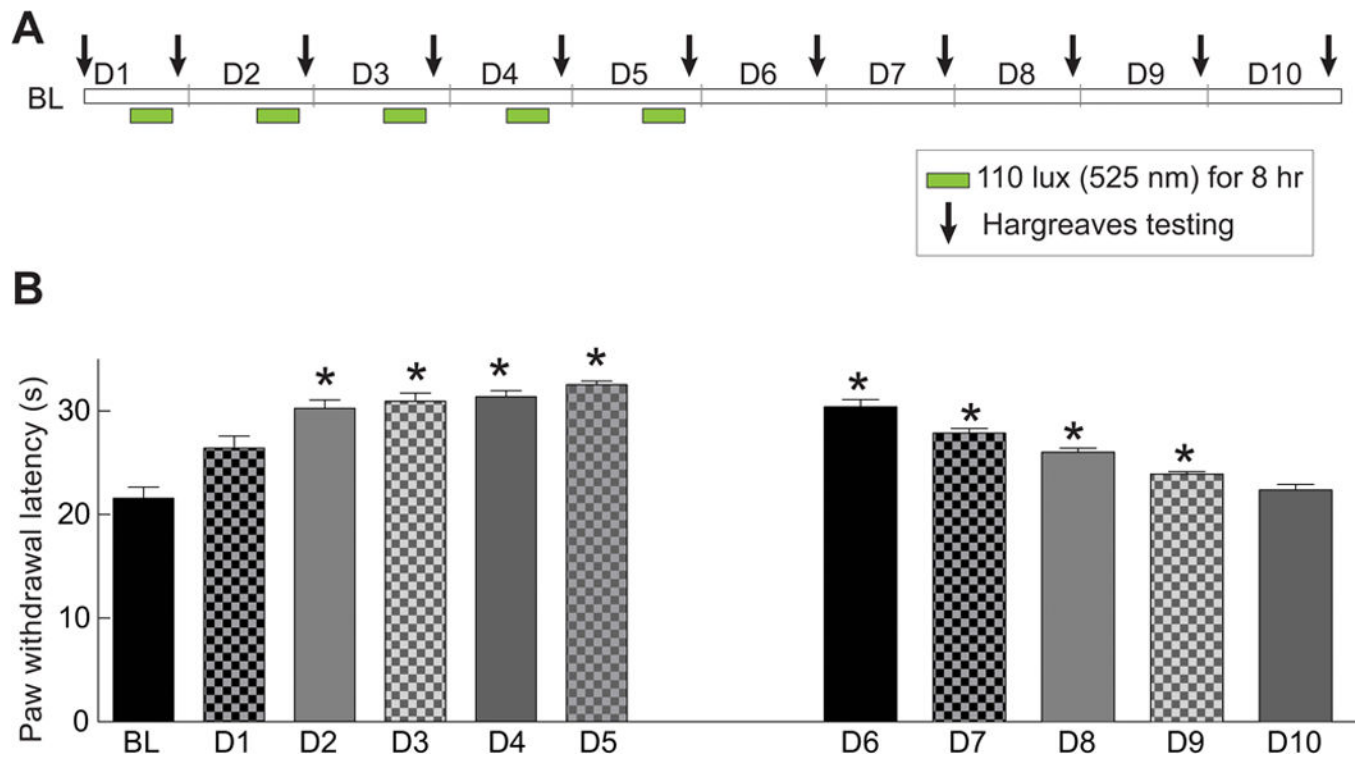
Figure 2. Green light emitting diode (GLED)-induced thermal analgesia – time course and duration of effect

(**A**) Schematic representation of the experimental design, LED exposures, and Hargreaves testing. (**B**) Bar graph showing the paw withdrawal latency (seconds) of rats (n=6 per group) treated as shown in the schematic in **A**. BL indicates the baseline latency before GLED exposure. GLED exposure resulted in thermal analgesia starting at the second day (D2) of phototherapy and lasted 4 days after cessation (till D9) of LED exposure. *p<0.05 when comparing to BL (one-way ANOVA followed by Student-Newman-Keuls test).
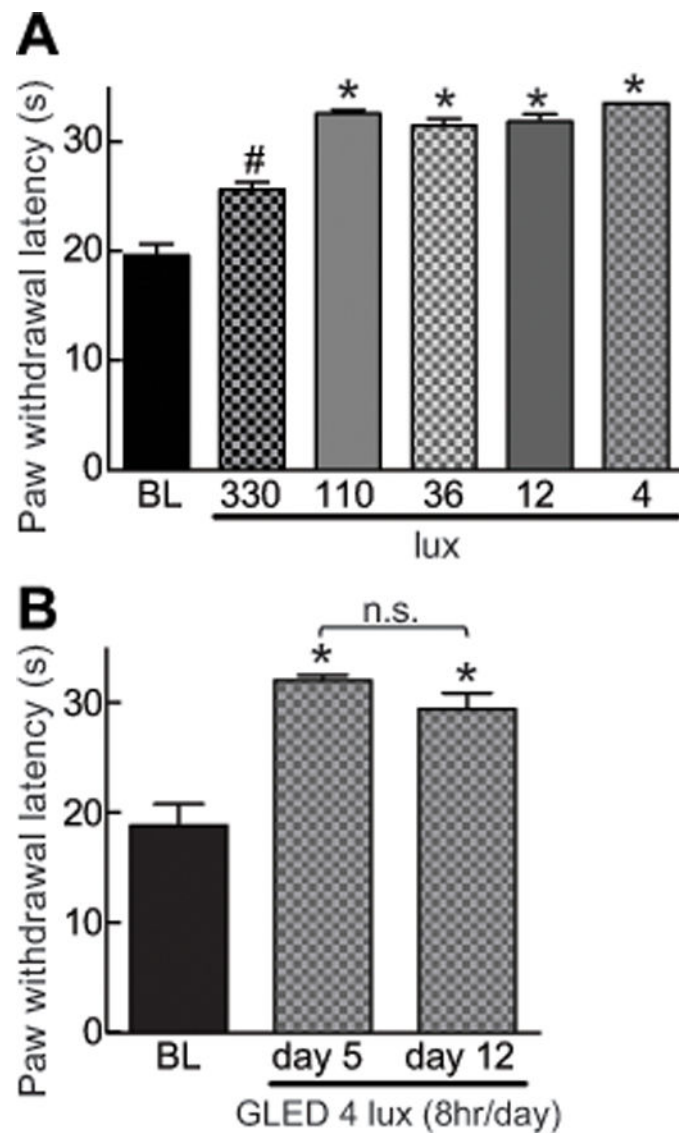
Figure 3. Green light emitting diode (GLED)-induced thermal analgesia – effect of level of illuminance – without development of tolerance

(**A**) Bar graph of paw withdrawal latency (PWL, in seconds) of rats (n=6 per group) exposed to the indicated illuminance level of GLED for eight hours daily for five days. BL indicates the baseline latency before GLED exposure. LED exposure GLED exposure as low as 4 lux resulted in thermal analgesia. (**B**) Bar graph of PWL (seconds) of rats (n=6 per group) exposed to the indicated illuminance level of GLED for eight hours daily for five and twelve days. The PWLs were not different following 5 and 12 days of consecutive exposure to GLED. *$p < 0.05$ when comparing to BL (one-way ANOVA followed by Student-Newman-Keuls test).
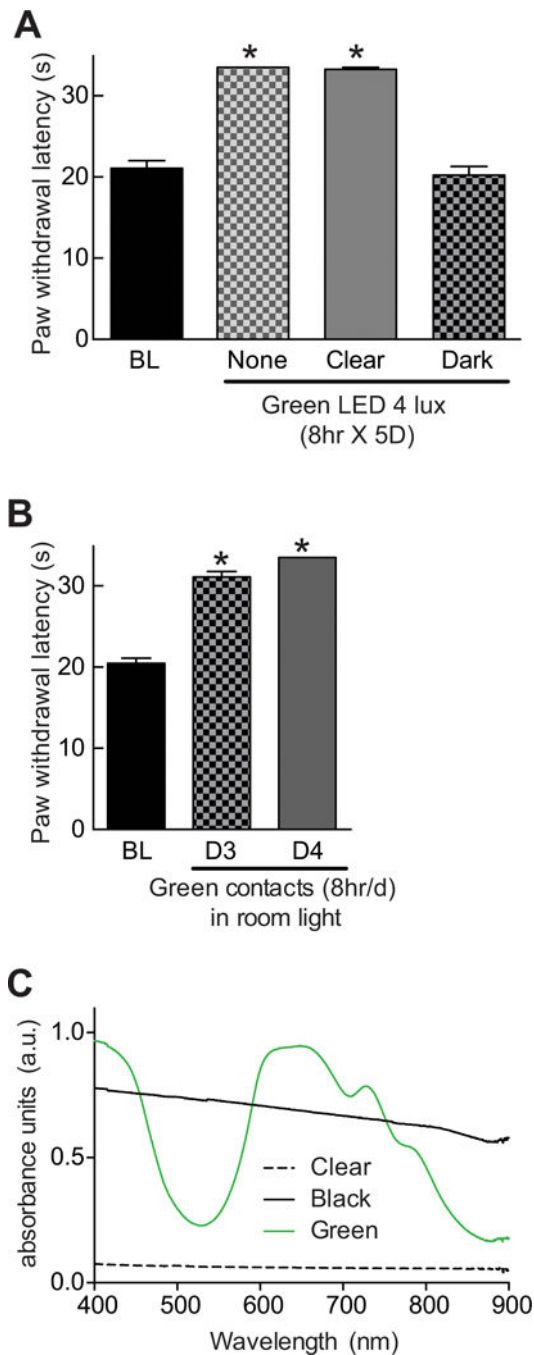
Figure 4. Involvement of the visual system in green light emitting diode (GLED)-induced thermal analgesia

(**A**) Bar graph of paw withdrawal latency (seconds) of rats (n=6 per group) prior to and after treatment with GLED as indicated. During the GLED exposure paradigm, the rats were fitted with clear or dark plastic lenses on their eyes. Blocking green LED absorbance to the eyes with dark contacts prevented the development of GLED-induced thermal analgesia. (**B**) Rats 'wearing' green plastic eye contacts and exposed to ambient room light for eight hours daily, developed thermal analgesia on days 3 and 4. *p<0.05 when comparing to baseline

(BL) (one-way ANOVA followed by Student-Newman-Keuls test). (**C**) Absorbance spectra, in arbitrary units (a.u.), of clear, dark, or green contacts. Dark contacts absorbed light in all wavelengths while green contacts showed a peak absorbance in the 580–700 nm range.
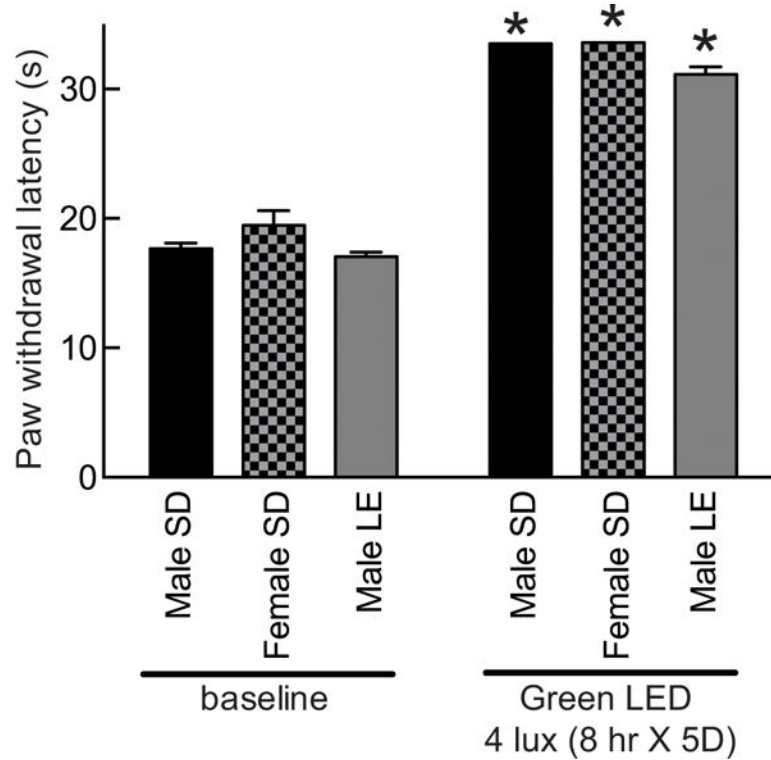
Figure 5. Green light emitting diode (GLED)-induced thermal analgesia does not rely on skin pigmentation and occurs in both genders

Bar graph of paw withdrawal latency (seconds) of male and female Sprague-dawley rats (SD, white fur) and male long-evans (LE) rats (n=6 per group) prior to and after treatment with GLED as indicated. All rats developed thermal analgesia compared to their own baseline. *p<0.05 when comparing to baseline (one-way ANOVA followed by Student-Newman-Keuls test).
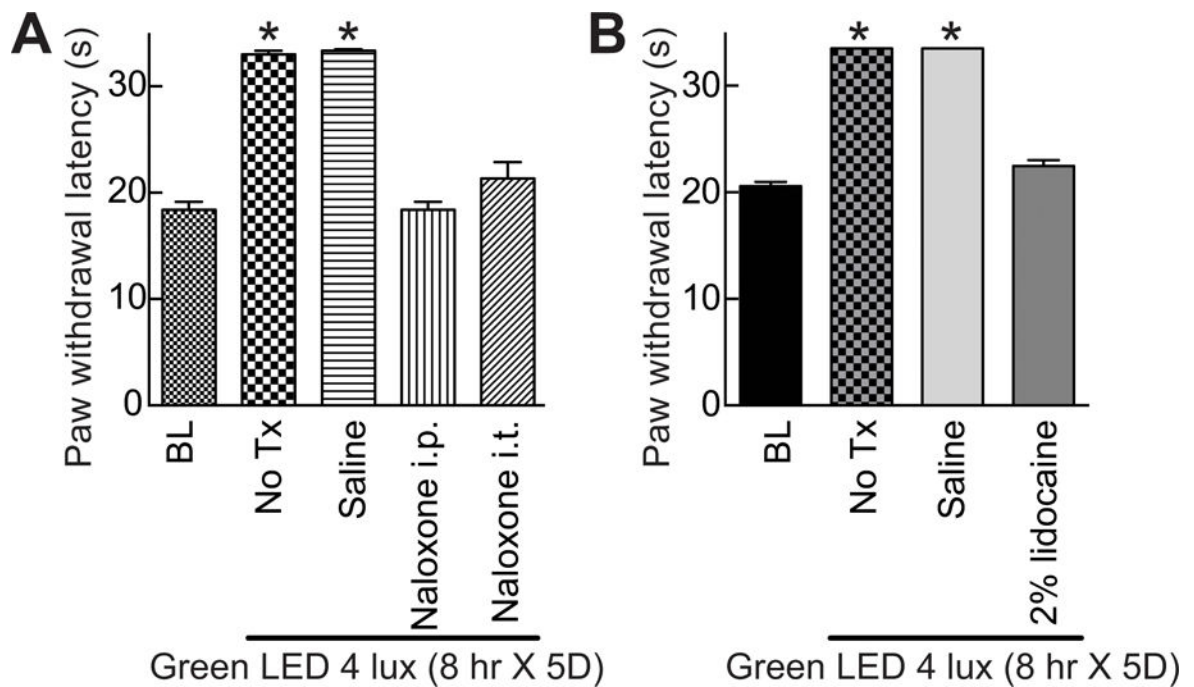
Figure 6. Green light emitting diode (GLED)-induced thermal analgesia involves activity of the descending pain pathways through endogenous opioid signaling

(**A**) Bar graph of paw withdrawal latency (seconds) of rats (n=6 per group) prior to and after treatment with GLED as indicated. BL indicates the baseline latency before GLED exposure. Inhibiting mu-opioid receptor (MOR) with naloxone (intraperitoneal (i.p.) or intrathecal (i.t.) administration) (see Table 1) reversed GLED-induced thermal analgesia. Un-treated (No Tx) rats or rats injected i.p. with saline (n=6 per group) developed GLED-induced thermal analgesia. (**B**) Inactivation of the descending pathway pain with an injection of a 2% solution of lidocaine into the rostral ventromedial medulla (RVM) of rats (n=6 per group) reversed GLED-induced thermal analgesia. *p<0.05 when comparing to BL (one-way ANOVA followed by Student-Newman-Keuls test).
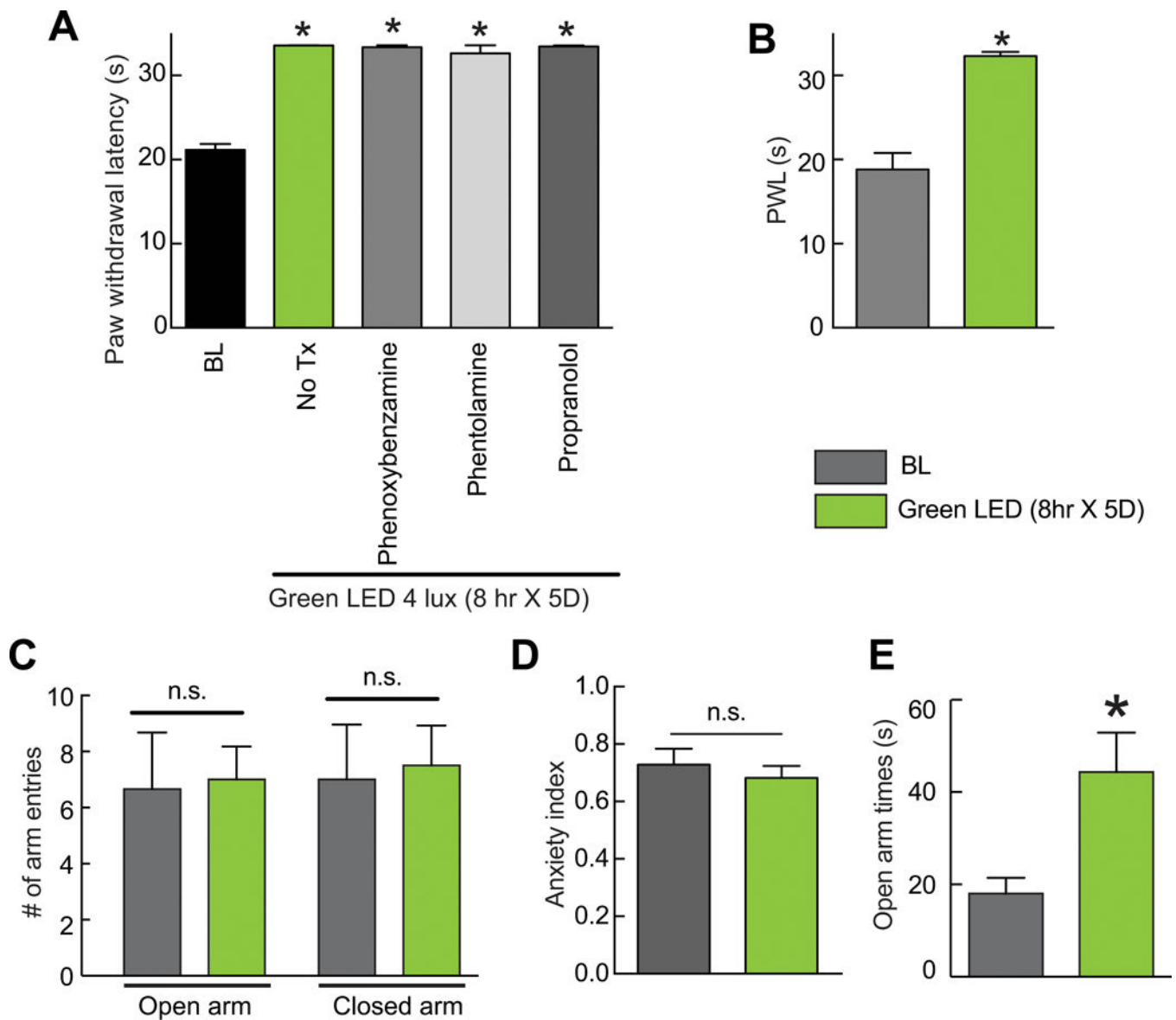
Figure 7. Green light emitting diode (GLED)-induced thermal analgesia does not invoke a stress/anxiety response

(**A**) Bar graph of paw withdrawal latency (seconds) of rats (n=6 per group) prior to and after treatment with GLED as indicated. BL indicates the baseline latency before GLED exposure. Inhibiting the alpha- (with Phenoxybenzamine or Phentolamine) or beta- (with propranolol) adrenergic receptors (see Table 1) failed to reverse GLED-induced thermal analgesia. (**B**) Following verification that GLED exposure (8 hr × 5D) induces analgesia (B), rats were subjected to the elevated plus maze (EPM) test. (**C**) GLED exposure did not change the number of times the rats entered the open or closed arms in the EPM. (**D**) The anxiety index, an integrated measure of times and entries into the arms of the EPM, was not different between rats at baseline and after exposure to the GLED paradigm. (**E**) The GLED exposed rats spent significantly more time in the open arms, indicating that GLED exposure

was anxiolytic. *p<0.05 when comparing to BL (one-way ANOVA followed by Student-Newman-Keuls test).
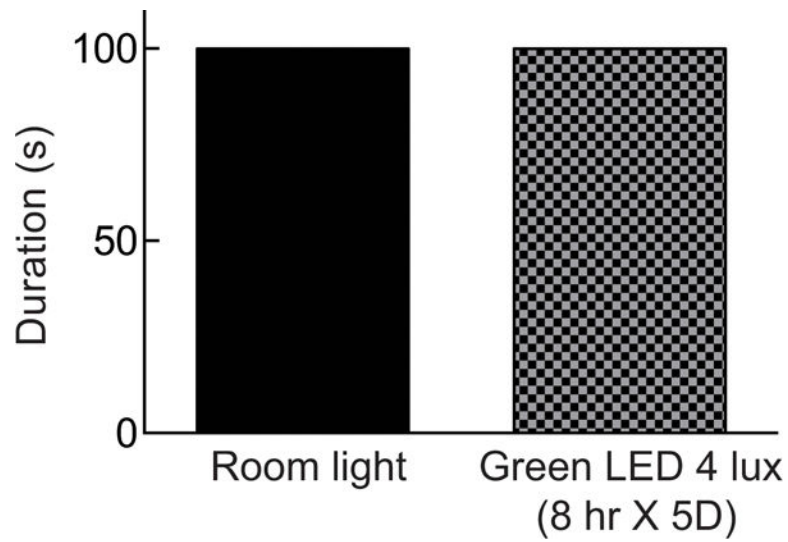
Figure 8. Motor function is not affected by green light emitting diode (LED) treatment
Bar graph of latency of rats (n=6 per group) to fall off the rotarod at incremental speed.
Thermal analgesia induced by GLED exposure did not impair motoric performance as there
were no differences between the fall off latencies between these and rats exposed to ambient
room light. p>0.05 when comparing between the two conditions (paired Student's t test).
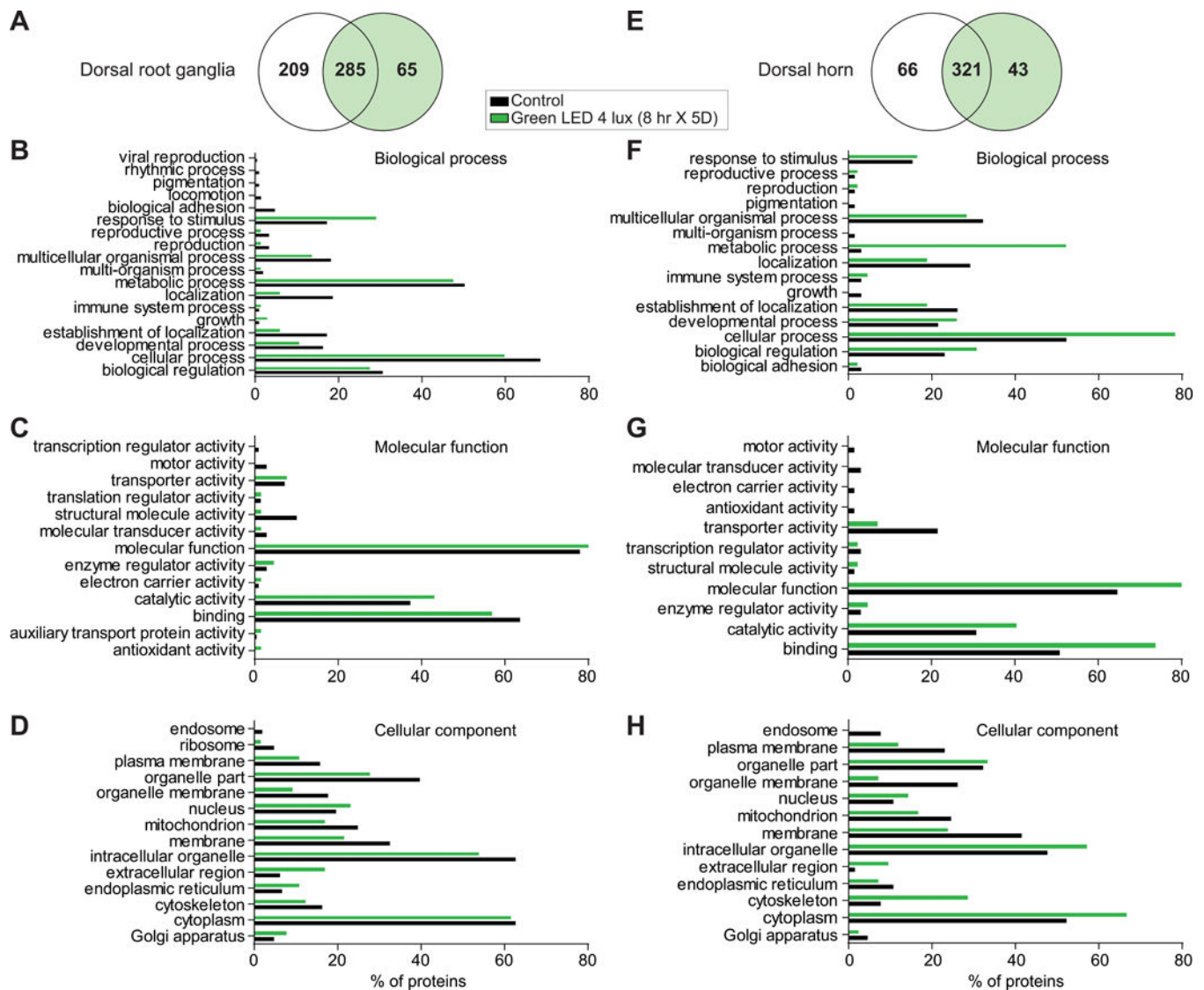
Figure 9. Comparative proteomic analysis of dorsal root ganglia (DRG) and dorsal horn (DH) of the spinal cord from rats exposed ambient or green light emitting diode (GLED) using one-dimensional-liquid chromatography-electrospray ionization-tandem mass spectrometry

Venn diagram of the identified proteins in control and GLED exposed rat DRG (**A**) and dorsal horn of the spinal cord (**E**). Biological process (**B**, **F**), molecular function (**C**, **G**), and cellular component (**D**, **H**) were analyzed using the Proteome software Scaffold. The numbers indicate the percent of proteins detected in the proteomic study that are clustered in the annotated groups from naïve (black) or GLED exposed rats (green).
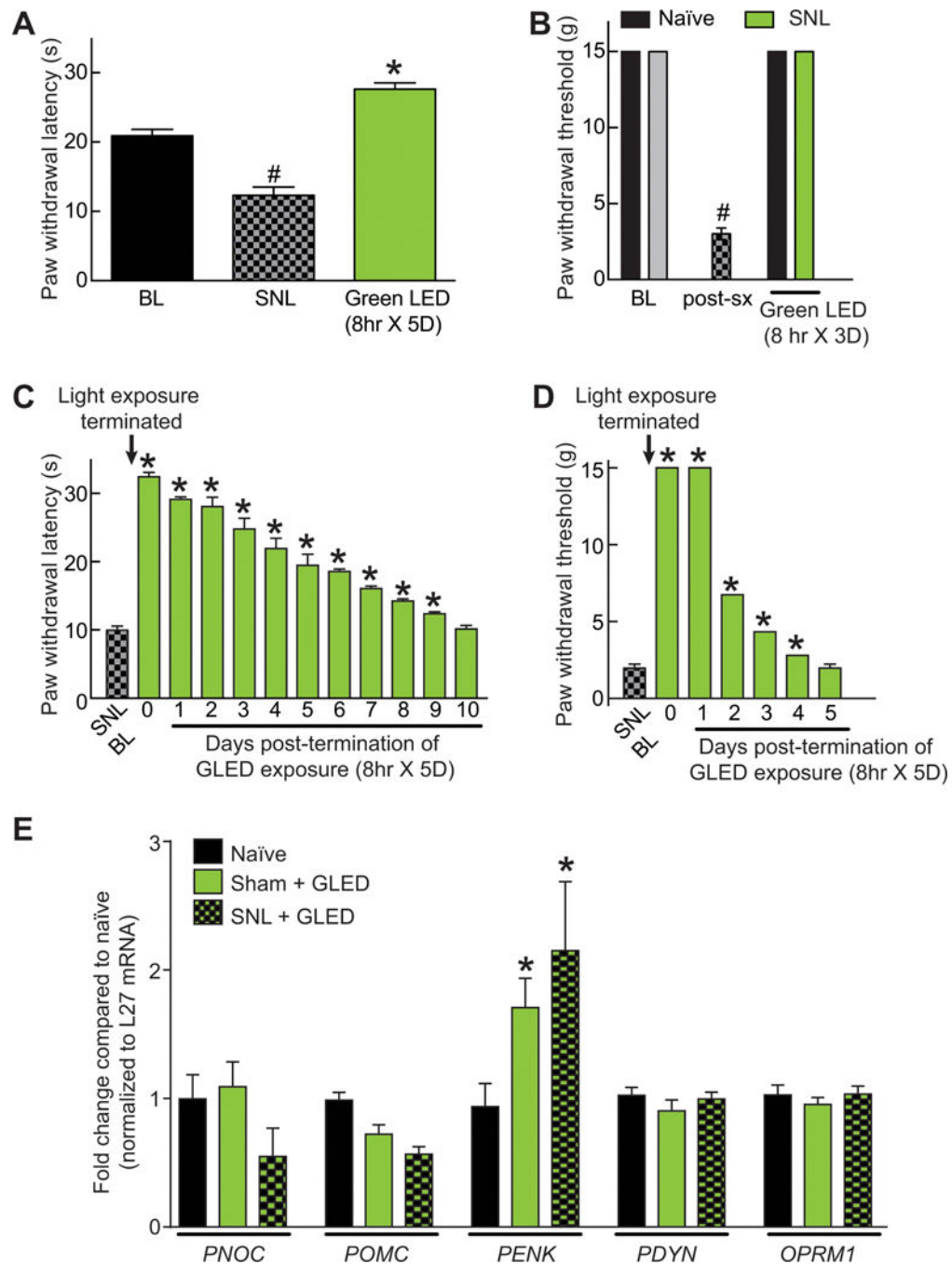
Figure 10. Exposure to green light emitting diode (GLED) reverses thermal hyperalgesia and mechanical allodynia induced in a model of neuropathic pain

(**A**) Seven days following a spinal nerve ligation (SNL) surgery on their left hind paw, rats (n=6 per group for all groups throughout this figure) displayed a significant decrease in their paw withdrawal latencies (PWLs, seconds), which was completely reversed by daily eight hours exposure to GLED exposure (4 lux). #p<0.05 when comparing to BL, *p<0.05 when comparing to BL or SNL (one-way ANOVA followed by Student-Newman-Keuls test). (**B**) Bar graph of paw withdrawal thresholds (PWTs, grams) of rats after receiving a SNL injury

and after GLED exposure for 3 days (4 lux, 8 hours per day). BL indicates the baseline PWT before GLED exposure. PWTs were completely reversed 3 days of GLED exposure compared to post-surgery (post-Sx) levels. #p<0.05 compared to BL (one-way ANOVA followed by Student-Newman-Keuls test). Time course of return to baseline for PWLs (**C**) and PWTs (**D**). Some error bars are smaller than the bars. (E) Quantitative RT-PCR for the indicated genes from spinal cords of naïve rats as well rats with SNL + GLED or Sham + GLED. The mRNA levels for each gene were normalized to L27 mRNA (a ribosomal internal control gene). The L27-normalized values for each condition were divided by the L27-normalized values for naïve and are expressed as fold change over naïve levels. Data represent mean fold change ± S.E.M. (n=3 for each). A robust upregulation of PENK mRNA was observed in SNL + GLED or Sham + GLED condition (*, p<0.05, Student's t-test vs. control).

Table 1

Experimental compounds used in this study.

Experimental compound	Vendor	Catalog number	Target/mechanism of action	Dose	Route
Naloxone	Tocris	0599	non-selective opioid receptors	20 mg/kg	Intraperitoneal (i.p.)
				20 µg	Intrathecal (i.t.)
Phentolamine	Sigma	P7547	beta-adrenergic receptor	3 mg/kg	i.p.
Propranolol	Sigma	P0884	beta1-/beta2- adrenergic receptor	10 mg/kg	subcutaneously (s.c.)
Phenoxybenzamine	Sigma	B019	alpha 1-adrenergic receptor	1 mg/kg	i.p.

Table 2

List of primers used for semi quantitative real time polymerase chain reaction

Gene name (rat)	Orientation	Sequence	Reference
PENK	Forward	CAGCTCTTTGGCTTCATCT	[18]
	Reverse	AGAGGCCAATGGAAGTGAGA	
POMC	Forward	AGGACCTCACCACGGAAAG	[11]
	Reverse	ACTTCCGGGGATTTTCAGTC	
OPRM1	Forward	AAATGAAAGGGATTGAAAGCACA	[60]
	Reverse	CTCACTGGGTGACCTTCTGAACT	
PDYN	Forward	CTGTCTCCTCCCATCTCTGC	[17]
	Reverse	TAGCTGCTCCAGGTGATGTG	
PNOC	Forward	CAGACAGGGAGGACATGGAT	
	Reverse	GGACTGCAAAGTGCAGACAA	
L27	Forward	ATCGCCAAGCGATCCAAGAT	[8, 48]
	Reverse	CACAGAGTACCTTGTGGGCA	

Table 3

Proteins enriched in tissues from rats exposed to green light emitting diodes.

Identified proteins	Gene Name	Accession number[1]	% sequence coverage	Pain implication
Dorsal root ganglia				
Carboxypeptidase	*ctsa*	Q6AYS3_RAT	12%	Enkephalin degradation [14]
Alpha-synuclein	*snca*	SYUA_RAT	46%	Expressed in laminae I, II, VII and X of the dorsal horn [81]
Microtubule-associated protein	*mapt*	F1LST4_RAT	19%	Lost in neuropathic pain [39]
Thioredoxin	*txn*	THIO_RAT	54%	Improves ziconotide induced analgesia [84] Expression is changed after surgery [23]
Stathmin	*stmn1*	STMN1_RAT	37%	Substrate for Cdk5 [70]
Acid ceramidase	*asah1*	A0A0G2K8T0_RAT	28%	Inactivating mutation in Farber disease (patients experience pain) [7; 86]
Haptoglobin	*hp*	A0A0H2UHM3_RAT	18%	Serum concentration decreased in abdominal pain in horses [66]
Cofilin 2	*cfl2*	M0RC65_RAT	46%	Phosphorylation is associated with hyperalgesia [45; 87]
Calretinin	*calb2*	CALB2_RAT	21%	Protects against TRPV1-mediated toxicity in pain-sensing neurons [64]
Lactoylglutathione lyase	*glo1*	LGUL_RAT	45%	Expression reduced in diabetic neuropathy [37] Catalyses the detoxification of Methylglyoxal, a positive regulator of TRPA1, upregulated during painful neuropathy [1]
Dorsal horn of the spinal cord				
Lactoylglutathione lyase	*glo1*	LGUL_RAT	54%	Expression reduced in diabetic neuropathy [37] Catalyses the detoxification of Methylglyoxal, a positive regulator of TRPA1, upregulated during painful neuropathy [1]
Purine nucleoside phosphorylase	*pnp*	PNPH_RAT	25%	Catalyses the breakdown of adenosine into inosine, which induces anti-nociception in the formalin test [57]
Aspartyl aminopeptidase	*dnpep*	Q4V8H5_RAT	17%	Catalyses angiotensin III synthesis which activates inhibitory pain descending pathways from the periaqueductal gray matter [65]
Cathepsin B	*ctsb*	Q6IN22_RAT	22%	Expressed in microglia during inflammatory pain [77]
Alpha glucosidase 2 alpha neutral subunit	*ganab*	D3ZAN3_RAT	14%	Deficiency causes Pompe disease with increased mild pain [27]

[1] Accession number is from Universal Protein Resource (UniProt)